A blood sampling microsystem for pharmacokinetic applications: Design, fabrication, and initial results

Tao Li,*[a] Adam Barnett,[a] Karen L. Rogers†[b] and Yogesh B. Gianchandani[a]

Received 28th May 2009, Accepted 10th September 2009
First published as an Advance Article on the web 12th October 2009
DOI: 10.1039/b910508e

This paper describes a microsystem for automated blood sampling from laboratory mice used in pharmacokinetic studies. Intended to be mounted as a "backpack" on a mouse, it uses a microneedle, reservoir, and an actuator to instantaneously prick the animal for a time-point sample, eliminating the need for a tethered catheter with large dead volume. The blood is collected by capillary effect through a 31–33 gauge microneedle (250–210 μm OD) into a ≈1 μL micromachined steel reservoir. The voice coil actuator provides a peak force of ≈300 mN, which amply exceeds the measured piercing force of mouse skin (*i.e.*, 60–85 mN for a 31-gauge needle with 12° bevel). The sampling system was tested *in vitro* using a mock vessel with adjustable pressure; the reservoir was filled in <0.15 s by a combination of the capillary effect and blood pressure. The system may also be used to sample interstitial fluid, but the absence of blood pressure makes it necessary to enhance the capillary effect of the needle. This is accomplished by either electropolishing the inner surface to make it more hydrophilic or using a polymer wire insert to increase the surface area. The steel surface of the reservoir is also coated with silicon oxynitride by plasma-enhanced chemical vapor deposition to improve its hydrophilicity. Blood from fresh bovine tissue was collected into the reservoir to simulate interstitial fluid sampling. *In vivo* tests on live, anesthetized mice resulted in successful collection of blood into the reservoir. The possible integration of the device in microanalytical systems and the device scalability for multisampling are discussed.

I. Introduction

Pharmacokinetics (PK) is the study of how a living organism transports and eliminates drugs, and is essential to pharmaceutical research. PK studies involve the administration of a drug to a laboratory animal such as a rodent and withdrawing a series of blood samples over time. The samples are then analyzed to quantify the drug and metabolite concentrations as a function of time.

The sample collections and transfers in a typical PK study can use either manual or automated approaches. The manual approaches involve repetitive procedures that are tedious and time consuming, making them impractical for time-resolved studies. Commercially-available automated sampling systems (*e.g.* DiLab AccuSampler®) use surgically-implanted catheters to obtain blood samples from a rodent. The catheter is connected to a processing system that automatically withdraws blood at set time points. However, such systems require the animal to be anesthetized for catheter insertion and tethered for the whole duration of multi-point blood collection, and are known to cause stress-related endocrine changes which can potentially affect the result of the study.[1] More importantly, the need for sample transfers and tube flushing set a lower limit of ≈100 μL on the sample size that must be withdrawn. This relatively large sample size prevents serial sampling in small animals, such as the mouse, where the blood volume is limited. A 20 g transgenic mouse has a total blood volume of only 1.7 mL, and a single 100 μL sample is therefore nearly 6% of the total blood volume, permitting only one sample to be obtained from a specimen. For a study that requires multiple samples at separate time points, it becomes necessary to use a separate mouse for each time point. This has a multiplicative effect: at least 3 mice are sacrificed for each time sample to account for variability between specimens. Thus, an eight time-point study typically consumes 24 mice. A technology that provides isolated 1–10 μL samples at each time point would allow a full PK profile to be obtained from a single mouse, which is scientifically desirable and saves animal resources. The recently-introduced DiLab AccuSampler® μ is designed to collect 5–50 μl blood samples,[2] but it still requires animal tethering and surgery for catheter insertion. Moreover, it is not compatible with microfluidic technologies to form a microanalytical (lab-on-a-chip) system that would permit the integration of *in vivo* microsampling, sample preparation, and analysis.

This paper proposes a system that can sample blood from a laboratory mouse in the ≈1 μL range,‡ eliminating the large dead and transfer volumes of conventional approaches. The system is designed to be worn as a "backpack" that pricks the animal with a microneedle at designated time points. Since the animal does not need to be tethered, the sample may be less affected by endocrine changes and the stress associated with other sampling

[a]*Department of Electrical Engineering and Computer Science, University of Michigan, 1301 Beal Avenue, Ann Arbor, MI, 48109-2122, USA. E-mail: litz@umich.edu; Fax: +734-763-9324; Tel: +734-615-7983*
[b]*Unit for Laboratory Animal Medicine, Medical School, University of Michigan, Ann Arbor, USA*
† Current Affiliation: BioResources, Wyeth Research, Collegeville, PA

‡ Portions of this paper appear in conference abstract form in ref. 3.

methods. The blood sample is drawn through the needle and into a biocompatible steel reservoir that could be interchanged for a microanalytical chip. A voice coil actuator is triggered to provide the piercing action of the microneedle into the skin at each sampling time point.

Microneedles have been previously fabricated from silicon,[4–7] polymers,[8] and stainless steel[9] for use in drug delivery and transdermal fluid sampling. For fluid sampling, the needle must at least penetrate through the stratum corneum layer of the skin into the dermis layer, which contains blood vessels and nerves. Sampling can then be accomplished using an integrated micropump or the capillary effect. Capillary effect sampling using a hydrophilic microcapillary is a simple, reliable and cost-effective alternative to micropump sampling. This approach has been demonstrated for body fluid sampling with an array of silicon microneedles[7] and biodegradable polymer needles.[8] Although these materials can be easily micromachined to form the needle shape and surface treated to provide high capillary effect, their brittleness makes them susceptible to fracture during skin insertion. Biocompatible stainless steels are more ductile and make better candidates for the application; however, untreated stainless steel is only slightly hydrophilic, and additional measures are necessary to support sampling by the capillary effect.

The system design and fabrication are described in section II. The experimentally-measured piercing force required for the mice and rats, and the available force from the actuator are described in section III(A). Fabricated microsystems were tested both *in vitro* and *in vivo*. The *in vitro* tests included blood vessel sampling using a mock vessel with adjustable internal pressure, and interstitial fluid sampling from bovine tissue. The *in vivo* tests were performed to collect whole blood from live mice. The *in vitro* and *in vivo* experimental results are discussed in sections III(B) and III(C), respectively, and are followed by discussions in section IV.

II. System design and fabrication

(A) System architecture

The scheme for *in vivo* microsampling of mouse blood is shown in Fig. 1. A miniaturized "backpack" positions the sampling microsystem at a target spot on the mouse. To make this backpack, a commercial mouse jacket (Lomir Biomedical, Inc.) can be modified with Velcro tape. The sampling system consists of a microneedle, reservoir, and an actuator. The actuator can be triggered to suddenly prick the animal with the microneedle for a single time-point sample. Fluid is collected through the needle into the reservoir by the capillary effect, and the actuator is then triggered in the reverse direction to retract the needle from the animal.

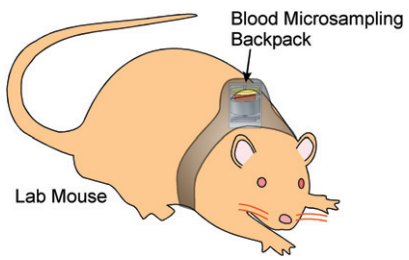

Fig. 1 Diagram showing application scheme of the blood sampling microsystem for pharmacokinetic studies.

The structure of the prototype system is shown in Fig. 2. A microneedle is mounted on a miniature blood reservoir with a target volume of 1–10 μL. The reservoir is covered with a glass lid that enables visual observation of the sample without opening the reservoir. An actuator, which provides the insertion and retraction movement of the needle and reservoir assembly, is integrated in a custom-designed Macor® ceramic housing. The top of the actuator is attached by an adjustable screw to the housing as shown in Fig. 2(a). With the proper needle and housing dimensions, a 2 mm deflection of the actuator can drive the needle 1 mm into the mouse through a hole in the ceramic housing. This depth can reach the mouse jugular in certain locations for vessel blood sampling.[10] Other insertion depths can be achieved by simply modifying the needle length and position of the adjustment screw for different sampling targets. The design considerations for each component in the system are provided in the following subsections.

(B) Needle and reservoir

Capillary draw is possible when adhesive forces between a solid surface and a liquid surface are stronger than the cohesive forces between the liquid molecules. For a cylindrical channel, the surface tension force that tends to draw liquid into the channel is[11]

$$F_t = 2\pi r\gamma_{lg}\cos\theta_c \quad (1)$$

where γ_{lg} is the surface tension at the liquid–air interface and r is the radius of the channel. θ_c is the contact angle between the liquid and the channel material. Its nominal value at equilibrium for a certain solid–liquid–gas interface is given by Young's equation

$$\cos\theta_c = \frac{\gamma_{sg} - \gamma_{sl}}{\gamma_{lg}} \quad (2)$$

where γ_{sg} and γ_{sl} are surface tensions at the solid–air and solid–liquid interfaces, respectively. As can be seen from eqn (2), $\theta_c \leq 90^\circ$ suggests that $\gamma_{sg} > \gamma_{sl}$. This causes the solid–liquid interface area to increase and results in a positive F_t which drives the flow in the channel.[12] When the channel is held horizontally, this force alone can drive the liquid to fill up the channel. When the channel is held vertically, the height, h, of the liquid column entering the channel is limited by the force of gravity, and is given by

$$F_t = G = \rho g h(\pi r^2) \Rightarrow h = \frac{2\gamma_{lg}\cos\theta_c}{\rho g r} \quad (3)$$

where G is the force of gravity on the liquid, ρ is the density of the liquid, and g is the acceleration due to gravity. As is clear from eqn (3), small θ_c and r are both desirable in order to enhance the capillary effect in the channel and increase the capillary height, h. These terms can serve as guidelines for the selection of the material and the dimensions of the microneedle.

Among the materials that have been used to form microneedles, silicon and polymeric materials can be easily surface treated to achieve a small θ_c for superior wettability, thus

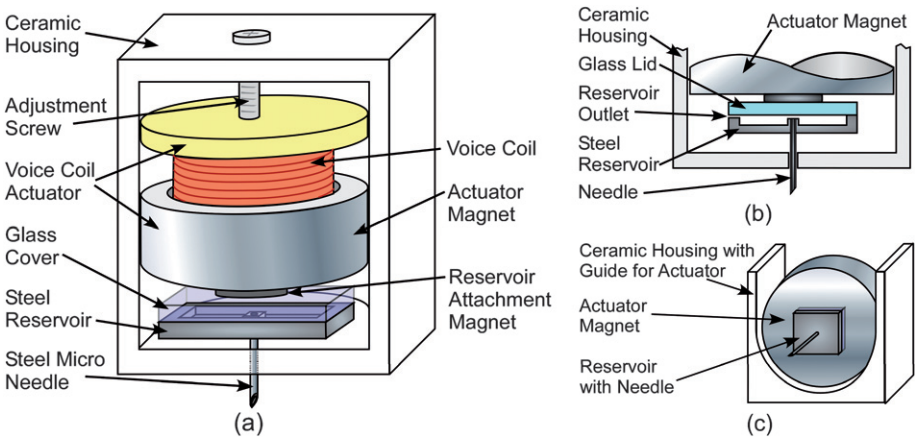

Fig. 2 Schematic diagram of the proposed system: (a) in front view; (b) cross-sectional view showing the reservoir; (c) showing the actuator and its guide on the Macor ceramic housing.

providing a strong capillary effect. These materials are also compatible with standard microfabrication technology and can be easily integrated with other micromachined devices for on-chip sample processing and analysis. However, these materials have relatively low strength and ductility, resulting in a high risk of fracture during skin insertion.[13] The structure of these needles must be carefully designed to withstand the skin piercing force.[6] Microneedle arrays can increase overall mechanical strength and fluid flow rate. However, arrays take up more space on the device and can push the skin down uniformly without penetrating it if the spacing between needles is too small.

Stainless steel has higher strength and is more ductile than silicon and polymeric materials, making steel needles safer and less prone to fracture during insertion. However, untreated stainless steel has only weak hydrophilicity, making it difficult to sample using the capillary effect. The contact angle, θ_c, of water on stainless steel depends on surface properties and the type of alloy.[14–16] Stainless steel 304 and 316L, which are the most commonly used alloys for hypodermic needles, are slightly hydrophilic and have a water contact angle of 50–70°. Needles made from these materials are used in this effort. However, surface treatments and other measures are employed to facilitate capillary draw. Note that while the contact angle of water is used to discuss the wettability of steels, the contact angle of whole blood has been shown to be similar.[14]

Various treatments have been proposed to improve the wettability of stainless steel by modifying the surface roughness, oxygen content, or organic contamination layer of the surface.[15–18] However, most treatments are either not permanent or are impractical to perform on the inner surface of a 31 or 33 gauge needle. Electropolishing is commonly used to clean stainless steel surfaces[19] and can be performed on the inner surface of a needle. This procedure decreases the roughness of the surface and removes any existing organic contamination layer, which has been shown to improve wettability.[15] A second approach to obtain a stronger capillary effect is to insert a hydrophilic wire into the needle. This wire serves as a "wick" by increasing the liquid-solid interface area. This additional surface area adds a second term to eqn (1):

$$F_t = 2\pi r_1 \gamma_{lg} \cos\theta_{c1} + 2\pi r_2 \gamma_{lg} \cos\theta_{c2} \quad (4)$$

where r_1 and r_2 are the radii of the channel and the wick insert, respectively; θ_{c1} and θ_{c2} are the contact angles between the liquid and the channel material and between the liquid and wick insert material, respectively. As shown in Fig. 3, a polymer-coated wire can be inserted into the needle for this purpose. The polymer is hydrophilic, and covers a copper core that can be reshaped so that the wire can stay inside the needle lumen after deployment. The top end of the wire touches the overhead glass lid, traversing a 50–100 μm gap. For example, this approach can provide ≈65% increase in F_t, assuming r_1 and r_2 are 130 μm and 50 μm, respectively, and the contact angle of water is 65° on clean stainless steel 304 and 45° on the polymer wire material.

Also shown in Fig. 3, an opening can be formed in the side wall of the microneedle near the tip. This feature is helpful during *in vivo* experiments by providing a second path for blood flow into the needle, especially if the needle tip is clogged by tissue during insertion.

The liquid entering the needle encounters a barrier at the joint of the needle and reservoir due to the discontinuity of the capillary surface. In the absence of an external pump, this barrier prevents the liquid from flowing into the reservoir cavity because of the liquid surface tension. As shown in Fig. 3, a simple solution is used for the prototype system by using wick fibers to guide the liquid from the needle exit into the reservoir and continue the capillary effect. Once the liquid from the needle tube reaches the

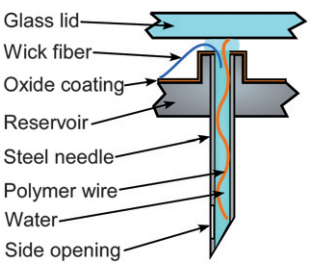

Fig. 3 Design variations used to improve capillary effect and *in vivo* sampling. A polymer wire is used as an insert in the needle tube to increase surface area; a wick fiber is used to guide liquid from the needle exit into the reservoir; an opening is formed on the side wall of the needle near the tip to prevent the needle lumen from being clogged by tissue during insertion.

highly hydrophilic surface of the glass lid and the reservoir, it is quickly drawn into and fills the reservoir. An alternative approach is to make a slanted wall forming a wedge angle at the needle exit to the reservoir. A properly designed wedge will cause the liquid to form a convex meniscus at the entry into the reservoir as discussed in ref. 12. The top of this meniscus would contact the hydrophilic glass lid surface 50–100 μm above the needle exit, continuing the capillary effect to drive the liquid into the reservoir. However, this approach requires a more complex microfabrication procedure especially due to the requirement of 3D micromachining of steels.

The volume of the reservoir can be designed to suit the requirements of different applications. A volume of 1 μL is demonstrated in this prototype. As shown in Fig. 2(b), the reservoir features a microchannel on one wall that permits air to leave the cavity during sampling. A side port can also be formed at the exit of the microchannel to allow the device to interface with additional components for *in situ* sample preparation and analysis. The reservoir is made from stainless steel to maintain consistency with the needle material, and can be replaced by others such as glass and polymer if needed for integration with other microfluidic devices to form a microanalytical system for an all-in-one solution for PK studies, as will be discussed in section IV. The inner surface of the steel reservoir is made highly wettable with a hydrophilic coating such as silicon oxide or oxynitride.

(C) Actuator

The actuator is triggered to insert the needle through the animal skin to a certain depth depending on the requirement of different sampling targets such as blood from vessels or interstitial fluid from the dermis layer.

During needle insertion, the outer epidermis layer of the skin poses the largest resistance force. The force on the needle increases with displacement of the needle as the skin is stretched, reaches a maximum, and then sharply decreases as the epidermis is pierced. The actuator must be able to supply at least this piercing force, which depends on the type of the skin and the needle tip diameter. Previous studies have measured the piercing force of human skin with surgical needles and microfabricated silicon needles to be <100 mN for a tip cross sectional area of <3000 μm^2.[13,20] The force required to puncture a blood vessel in a rabbit ear with a 400 μm diameter hypodermic needle was measured to be 151 mN.[21] The piercing force of mouse skin is difficult to estimate from these results due to the differences in thickness and elasticity. However, it is expected to be less than that of human skin because the mouse epidermis is only 9.1–13.7 μm thick, while the human epidermis is 60–130 μm.[22] Experiments were conducted to measure the piercing force of the stainless steel needle into mouse and rat skin to examine the feasibility of the actuator selection.

The rough upper bound of 100 mN for the piercing force is one guideline for the actuator selection, and the other requirement is that the actuator must provide a stroke >3 mm. The travel distance of the actuator determines the insertion depth of the needle, and a stroke of this magnitude is necessary to reach the dermis layer of mouse skin or deeper for different sampling targets. For practical use, needle insertion depth should also be adjustable so that the microsystem can be used for different targets. Voice coil electromagnetic actuators are chosen for the prototype to meet both requirements. Compared with piezoelectric and electrostatic actuators, these magnetic actuators can easily provide the desired force and stroke with a compact size and low driving voltage.

As shown in Fig.2, a commercial voice coil actuator (H2W Technologies, Inc., USA) is selected for the system and integrated into the Macor ceramic housing, which also guides the motion of the actuator magnet. A separate rare earth magnet is used to bond the glass cover of a sampling reservoir to the actuator magnet for easy attachment or removal of the reservoir. The actuator has a nominal peak force of 300 mN and a stroke of 3.2 mm, meeting both the force and insertion depth requirements. The magnet for the reservoir attachment also enhances the actuator performance by increasing the strength of its magnetic field, and will be verified with experiments in section III(A).

(D) Reservoir fabrication

The fabrication steps for the sampling system are shown in Fig. 4. The reservoir is made from a 500 μm-thick, biocompatible stainless steel 304 plate using micro electrodischarge machining (μEDM). The SEM image of a fabricated 1 μL reservoir is shown in Fig. 5(a). The cavity is 300 μm deep with a 2.3 mm square interior footprint, and features a 600 μm-square, 200 μm-tall protruding inlet at the center for needle attachment. An optional side port, which can be used for interfacing to external sample processing components, is also shown in the figure. The reservoir is then coated with silicon oxide or oxynitride using plasma-enhanced chemical vapor deposition (PECVD) to obtain a hydrophilic surface. The steel microneedle is formed by using μEDM to re-work either of two types of commercial needles: a 33-gauge needle (210 μm OD, 115 μm ID) from World Precision Instruments (WPI), Inc. (Fig. 5b), and a 31-gauge needle (250 μm OD, ≈130 μm ID) from Becton Dickinson (BD). The capillary draw of the needle is enhanced by either electropolishing or inserting a polymer-coated wire as discussed in section II(B). For electropolishing, a method discussed in ref. 19 is used to enhance the hydrophilic property of the inner surface of the needle, with the outer surface protected from the solution by a curable polymer coating (cyanoacrylate-based adhesive,

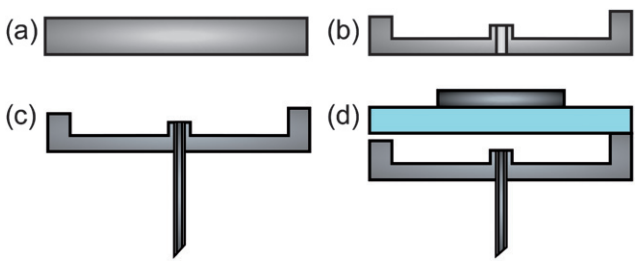

Fig. 4 Fabrication process for the reservoir: (a) the process starts with a biocompatible stainless steel 304 plate; (b) reservoir features are fabricated on the plate by μEDM; (c) the microneedle with μEDM'ed side opening is attached to the reservoir using polymer; (d) the glass lid and the magnet for actuator attachment is mounted using polymer after any wire insert and wick fiber are deployed.

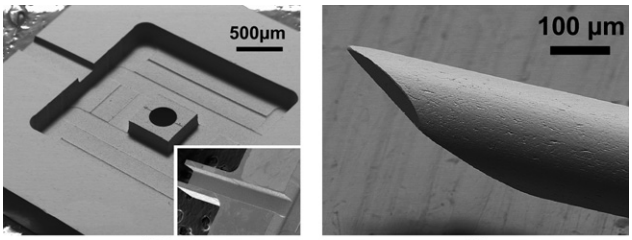

Fig. 5 SEM images of: (a) the μEDM'ed reservoir showing a shallow channel on the wall for air exit and an optional exit connector with a deeper channel for external devices for sample processing; cavity volume ≈ 1.0 μL. (b) The tip of the 33-gauge needle; outer diameter = 210 μm; inner diameter = 115 μm.

Henkel Corporation). This method utilizes commercially-available EPS4000, which is a mixture of phosphoric and sulfuric acid. The needle is then attached to the reservoir using the same curable polymer. The 500 μm-thick glass lid and 3 mm-diameter rare earth magnet are then mounted onto the reservoir also using the curable polymer (Fig. 6a), leaving a 50–100 μm gap between the top end of the needle and the glass lid for blood inflow. The assembled reservoir is then attached to the actuator magnet and mounted in the custom-machined Macor® ceramic housing. The housing has dimensions of 23.9 (L) × 15.2 (W) × 13.7 (H) mm, and has a 250 μm-diameter hole on the bottom sidewall for the needle. The assembled system is shown in Fig. 6(b).

III. Experimental results

(A) Actuator evaluation

The piercing force of mouse skin depends heavily on the needle tip size and bevel shape, and experiments were carried out to characterize the piercing force of the BD 31-gauge microneedle with regular 12° bevel into fresh mouse carcasses. The carcasses were located on a motorized stage and fed toward a testing needle. The needle was mounted on a force gauge and measured force data were recorded on a computer. Fig. 7(a) shows the recorded force data during a single insertion into the skin of the mouse. As expected, the force increases in the beginning as the skin deflects, reaches a maximum when the skin is pierced, and then sharply decreases to a lower stable value which corresponds to the friction force between the needle shank and the tissue. The measurement was repeated at different locations of the mouse body including back, side and abdomen, at varying feeding speeds ranging from 50 μm s^{-1} to 750 μm s^{-1}, using either fresh or used needles. Tests were also repeated on a second mouse carcass to account for variability. As shown in Fig. 7(b), the piercing force with a fresh needle varies between 60–85 mN, while with a used needle it rises to 110–130 mN. This force does not vary much with different feeding speed, or at the three locations on the mouse body. The measured piercing force is much larger than is estimated using empirical equations for silicon microneedles from ref. 13, or experiments on silicon rubber, which is an artificial skin material with mechanical properties similar to human skin.[3,23] The testing results were used as a design guideline for actuator selection. The piercing force of rat skin was also tested, and was found to be 170–190 mN with a fresh needle and 260–300 mN with a used needle.

The force supplied by the commercial voice coil actuator is also measured using the force gauge. The results shown in Fig. 8 indicate that the actuator amply exceeds the piercing force requirement for mouse skin when the supplied current is more than ≈200 mA (≈0.4 V). The additional reservoir attachment magnet provides a ≈30% enhancement due to an increase in the magnetic field within the actuator, reaching ≈170 mN with 360 mA applied at a displacement of ≈1 mm. A maximum force of ≈300 mN can be obtained at about ≈1 mm displacement with ≈620 mA (≈1.4 V) supplied, and quickly drops when the displacement becomes larger. The generated force over the entire stroke of the actuator remains greater than ≈85 mN when the supplied current is more than ≈480 mA (1 V).

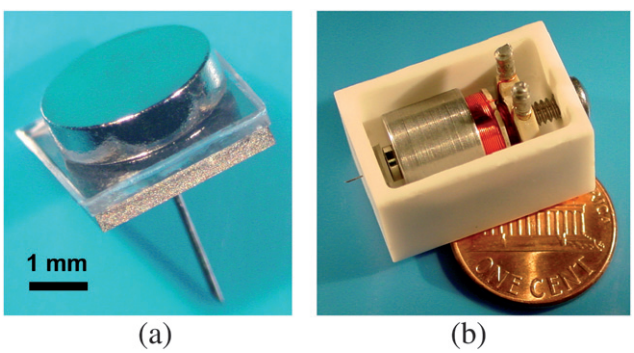

Fig. 6 Photos of: (a) the assembled reservoir with glass lid and attached magnet; (b) the full sampling microsystem. A glass cover can be used to seal the ceramic housing.

(B) *In vitro* experiments

The assembled system was first tested *in vitro*: (i) using pressure-driven flow, with the presence of unenhanced capillary forces; (ii) using capillary-driven flow, unassisted by a pressure differential along the needle. The first test was designed to study the fluidic characteristics of the system when sampling from a blood vessel, while the second test was performed to evaluate the sampling system before and after the modifications to enhance capillary effect, and the feasibility of using the system for interstitial fluid sampling.

(i) Pressure-driven flow. The experimental setup shown in Fig. 9(a) is built to evaluate the capability of the system to sample blood from a vessel, *e.g.* the jugular vein. A 4 mm-long needle (WPI 33-gauge) that has not been enhanced for capillary draw is inserted into the mock vessel. The mock vessel contains water instead of blood, and can be pressurized by a hand pump. This substitution is further discussed in section IV. Due to the weakly hydrophilic nature of the inner surface of the needle, the capillary effect does not, by itself, draw liquid into the needle. A pressure threshold of ≈29.0 mmHg is necessary to permit water flow through the needle. Once the water reaches the highly hydrophilic glass lid, the reservoir quickly fills by a combination of pressure-driven flow and the capillary effect. This pressure threshold is much smaller than mouse blood pressure (125 mmHg

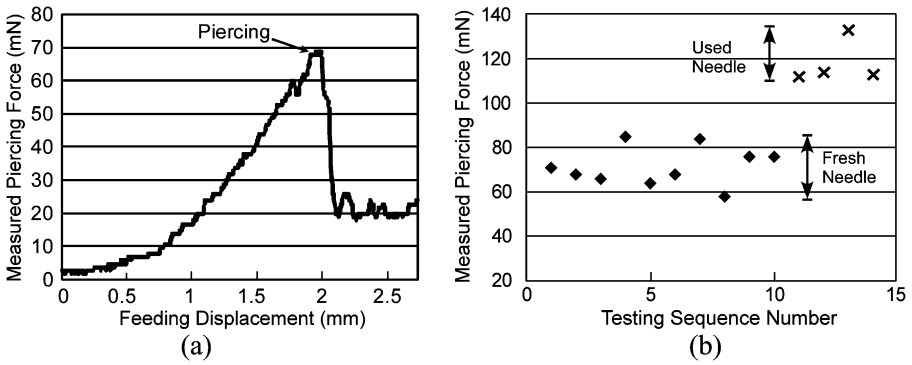

Fig. 7 Measurement results of the piercing force of BD 31-gauge needles into mouse skin: (a) force data recorded during a single insertion showing the peaking force at piercing; (b) distribution of multiple measurement results using either fresh needles or needles that have been used.

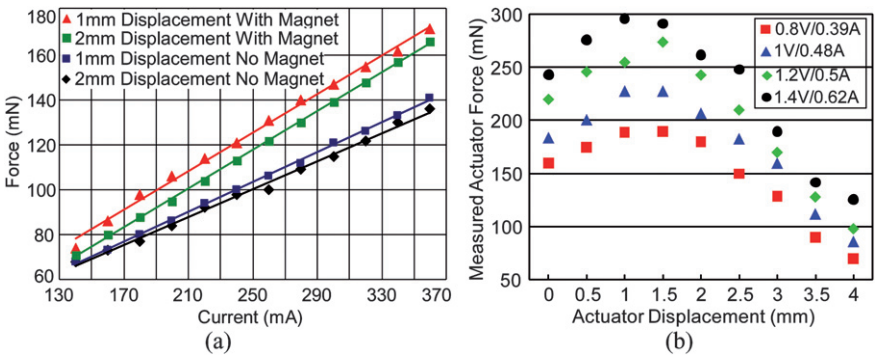

Fig. 8 Measurement results of the supplied force from the voice coil actuator. (a) Measured force *vs.* supplied current at certain displacement. The actuator force is enhanced by ≈30% with the presence of the magnet for reservoir attachment. (b) Measured force *vs.* actuator displacement at certain supplied current.

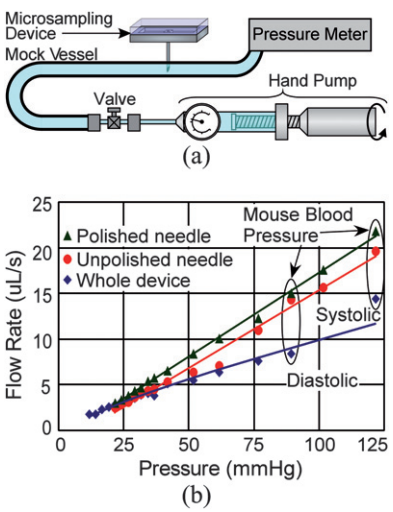

Fig. 9 (a) Schematic of testing setup for blood sampling from mock vessel. (b) Results showing measured flow rate *vs.* applied pressure through the whole device, a polished and an unpolished needle.

systolic, 90 mmHg diastolic[24]), so additional surface treatment to enhance the capillary effect is unnecessary for vessel sampling. At either pressure, systolic or diastolic, it takes <0.15 s to fill the reservoir.

The flow rate through the needle, reservoir, and a pipe of 600 μm ID attached at the reservoir outlet, was measured to study the capability of the device to deliver liquid to microfluidic components for *in situ* sample analysis. Fig. 9(b) shows this flow rate through the whole device as a function of "vascular" pressure in the mock vessel. The resulting flow rate is adequate for many microfluidic applications.

(ii) Capillary flow. Two approaches, discussed in section II, were used to enhance capillary flow, as would be required to sample interstitial fluids. The first approach, electropolishing with the EPS4000 solution, was first tested on a bare stainless steel 304 sample. The water contact angle improved from ≈94° before polishing and cleaning to ≈34° after polishing, indicating the improved wettability of the electropolished surface. The inner surface of the WPI 33-gauge microneedles were then electropolished by EPS4000. A typical polished surface is shown in the SEM images in Fig. 10. The capillary effect was tested and is compared in Table 1. After polishing, the capillary effect raises the water level in a vertical needle by ≈4 mm and fills a 10 mm horizontal needle in ≈1 s, the difference being caused by gravity. The 4 mm height is sufficient to fill the needle in the present design.

To evaluate the effect of polishing on flow rate at a given pressure differential, a 25 mm-long needle was tested with the setup in Fig. 9(a) before and after electropolishing. The results

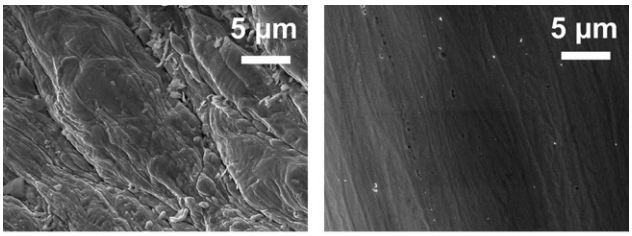

Fig. 10 SEM images of the needle inner surface: (a) before electropolishing; (b) after electropolishing using EPS4000. A slot opening was cut on the needle tube using μEDM before taking the SEM images.

Table 1 Capillary effect of the 33-gauge needle

	Unpolished	Polished
Water height in vertical needle	≈0	≈4 mm
Time to fill a 10 mm-long horizontal needle	>3 s	≈1 s

shown in Fig. 9(b) have been scaled to match the 4 mm length of the needle in the sampling system, and indicate a clear increase in flow rate with the polished inner surface and increased inner diameter of the needle.

Although the eletropolishing approach effectively improves the capillary effect, there are a few challenges in polishing the inner surface of needles. These include limited polishing efficiency and uniformity due to higher current density at the two opening ends of the needle compared with the inner surface towards the center.

The second approach uses a 50 μm-diameter polymer wire inserted into the needle tube to increase surface area for capillary effect. Experiments showed that this scheme can easily raise the water level to fill a 25 mm-long needle tube that is positioned vertically.

To compare different PECVD silicon oxide and oxynitride layers as the hydrophilic coating on the inner surface of the reservoir, water contact angles were measured on a stainless steel 304 surface with different coatings and results are shown in Table 2. According to the measurements, the cleaned bare stainless steel 304 surface has a fairly large water contact angle of 64–68°. After coating with oxide or oxynitride layers, the measured contact angles dropped, and the low-stress oxynitride coating provided the lowest contact angle (15–21°). This coating material has an index of refraction of 1.5, suggesting its

Table 2 Results of contact angle measurement for different stainless steel 304 (SS304) surfaces with and without oxide or oxynitride PECVD coatings

Surface type	Deposition T/°C	Coating thickness/μm	Measured contact angle/°
Cleaned bare SS304	—	—	64–68
Low-stress oxynitride	400	5	15–21
Oxynitride	400	5	26–28
Oxide	200	2	25–31
Oxide	380	2	50–53

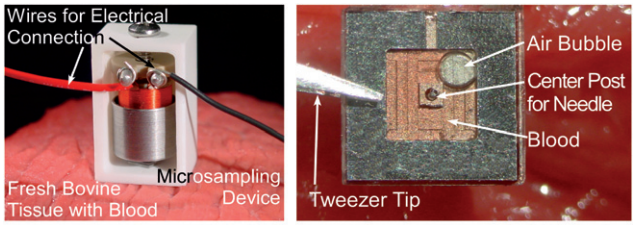

Fig. 11 Experiments with bovine tissue to explore the possibility of sampling interstitial fluid. (a) Photo of the system placed on the tissue sample for experiment. (b) Photo of the obtained blood sample in the reservoir with a small air bubble.

structural, optical and thermal characteristics are closer to those of oxide than of nitride.[25] The coating is called low stress because of its zero residue stress on a silicon substrate after deposition. It stays well on the steel substrate without peeling off, and is selected to coat the reservoirs.

To explore the possibility of sampling interstitial fluid rather than blood from vasculature, the sampling system with modified needle and reservoir were tested with bovine tissue samples. Fig. 11 shows the reservoir is almost completely flooded, leaving a small bubble of air.

(C) *In vivo* experiments

In vivo tests were performed on the microsystem using laboratory mice for blood sampling. The BD 31-gauge needles with polymer wire insert and side opening near the tip (Fig. 12a) were used for these tests. The reservoirs were coated with PECVD oxynitride, and wick fibers were used to guide fluid from the needle exit into the reservoir. The animals were anesthetized to simplify device mounting and testing, but this is not required for the normal operation of the automated sampling system. Tested sampling locations include mouse back, abdomen, thigh, and neck regions, and target skin spots were shaved and cleaned with antiseptic and alcohol. For testing convenience at multiple sampling locations, the system, with a ceramic housing, is manually held against the shaved skin of the anesthetized mouse. The actuator drove the needle into the mouse body when operated with >400 mA (0.8V) current, and after a sampling time of 1–2 s, which was empirically determined, it was triggered in the opposite direction to retract the needle from the mouse body. Blood was collected into the

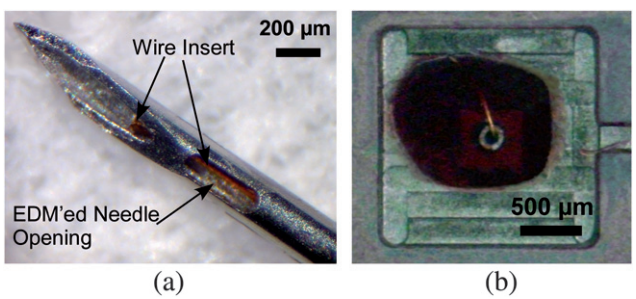

Fig. 12 Photos of: (a) μEDM'ed BD 31-gauge needle with a side opening and a polymer wire insert; (b) blood collected into the reservoir from live mouse body using a sampling system with a modified needle.

reservoir from all sampling sites, and a reservoir with collected blood is shown in Fig. 12(b).

IV. Discussion

It is worthwhile to consider system integration and scalability. As noted in section II, the present version of the microsampling reservoir has a side port for convenient sample transfer to microanalytical modules such as microfluidic components for sample concentration, separation and analysis. The external components can also be fabricated on the same substrate as the sampling reservoir, further reducing dead sample volumes caused by large interconnection distances between devices. Stainless steel is a promising substrate material for microfluidic devices, especially for reactors and mixers.[26] With the lithographic pattern transfer capability provided by batch mode μEDM,[27] implementation of microfluidic devices with complex patterns on this type of substrate is feasible. However, the more commonly used materials for microfluidic devices, such as glass and polymers, can also be used to fabricate sampling reservoirs for ease of integration. In the long term, it is possible to envision a system that provides complete *in situ* blood sampling and analysis for a PK profile.

As discussed in section I, a complete PK study involves multisampling from the animals to monitor the change in drug concentration over time. As the microsystem size is scaled down in the future, a method must be devised to array the sampling needles and reservoirs, to accommodate multiple time-point samples to be taken by a single assembly. An assembly of this type may require several microactuators, or a single actuator that is repositionable. For use with animals other than mice, the actuator would also have to provide the necessary force and displacement.

During the *in vitro* testing of the sampling system, water was used instead of blood. As mentioned in section II, the contact angles of water and whole blood are similar, and thus the results are reflective of the qualitative behavior that is expected with blood. The fluidic properties of blood plasma, which is mostly composed of water, are also comparable to those of water. However, the blood cells, which make up almost half of the whole blood by volume, are expected to result in a higher viscosity and thus slower flow rate through the sampling components than does the water. Further investigations would be necessary if the system is to be used for blood vessel sampling and driving additional fluidic components.

As noted in section III, the *in vivo* tests were performed on anesthetized animals. In order to extend this work to active animals, it may be necessary to develop a comfortable and secure harness for extended use. For small animals, it will also be helpful to further reduce the size and weight of the apparatus. This may require the development and use of customized actuators. (Micromachined actuators could present viable options.) An integrated power supply may also be needed.

V. Conclusions

A microsystem for automated sampling of blood is fabricated and evaluated using *in vitro* studies and *in vivo* studies with anesthetized mice. The system uses a 31–33 gauge needle and a reservoir with $\approx$1 μL volume, reducing the minimum sample size. It can help to substantially reduce the quantity of blood sampled and the number of animals sacrificed in an extended time point study. The research effort highlights system-level considerations, identifying challenges in actuator force and displacement, needle and reservoir hydrophilicity, and system integration, and presents potential solutions for each of these challenges.

Acknowledgements

The authors gratefully acknowledge Dr. Min Zhong of Pfizer Global Research and Development for providing the motivation and encouragement for this project. This work was supported primarily by the Engineering Research Centers Program of the National Science Foundation under Award Number EEC-9986866. Facilities used for this research include the Lurie Nanofabrication Facility (LNF) operated by the Solid-State Electronics Laboratory (SSEL), and animal facilities at the Medical School at the University of Michigan.

References

1 F. Royo, N. Björk, H.-E. Carlsson, S. Mayo and J. Hau, Impact of chronic catheterization and automated blood sampling (Accusampler) on serum corticosterone and fecal immunoreactive corticosterone metabolites and immunoglobulin A in male rats, *J. Endocrinol.*, 2004, **180**, 145–153.

2 DiLab website, http://www.dilab.com.

3 T. Li, A. Barnett, D. Xiao, M. Zhong, and Y. B. Gianchandani, "An in vivo blood microsampling device for pharmacokinetic applications," *Proc. Intl. Conf. Solid-State Sensors, Actuators and Microsystems (Transducers 2007)*, Lyon, France, 2007, pp. 225–228.

4 H. J. G. E. Gardeniers, R. Luttge, E. J. W. Berenschot, M. J. de Boer, S. Y. Yeshurun, M. Hefetz, R. van't Oever and A. van den Berg, Silicon micromachined hollow microneedles for transdermal liquid transport, *J. Microelectromech. Syst.*, 2003, **12**(6), 855–862.

5 P. Griss and G. Stemme, Side-opened out-of-plane microneedles for microfluidic transdermal liquid transfer, *J. Microelectromech. Syst.*, 2003, **12**(3), 296–301.

6 B. Stoeber and D. Liepmann, Arrays of hollow out-of-plane microneedles for drug delivery, *J. Microelectromech. Syst.*, 2005, **14**(3), 472–478.

7 E. V. Mukerjee, S. D. Collins, R. R. Isseroff and R. L. Smith, Microneedle array for transdermal biological fluid extraction and in situ analysis, *Sens. Actuators, A*, 2004, **114**(2–3), 267–75.

8 S. Aoyagi, H. Izumi, Y. Isono, K. Makihira, and M. Fukada, "Biodegradable polymer needle having a trench for collecting blood by the capillary force," *Proc. IEEE Intl. Conf. Micro Electro Mechanical Systems (MEMS 2006)*, Istanbul, Turkey, Jan. 2006, pp. 450–453.

9 A. Oki, M. Takai, H. Ogawa, Y. Takamura, T. Fukasawa, J. Kikuchi, Y. Ito, T. Ichiki and Y. Horiike, Healthcare chip for checking health condition from analysis of trace blood collected by painless needle, *Jpn. J. Appl. Phys.*, 2003, **42**, 3722–3727.

10 J. Hoff, Methods of blood collection in the mouse, *Lab Animal*, 2000, **29**(10), 47–53.

11 I. M. Cohen and P. K. Kundu, *Fluid Mechanics*, Elsevier Academic Press, San Diego, CA, 2004, pp. 8–12.

12 P. F. Man, C. H. Mastrangelo, M. A. Burns, D. T. Burke, "Microfabricated capillarity-driven stop valve and sample injector", *Proc. IEEE Intl. Conf. Micro Electro Mechanical Systems (MEMS 1998)*, pp. 45–50, January 1998.

13 S. P. Davis, B. J. Landis, Z. H. Adams, M. G. Allen and M. R. Prausnitz, Insertion of microneedles into skin: measurement and prediction of insertion force and needle fracture force, *J. Biomech.*, 2004, **37**, 1155–63.

14 S. Agathopoulos and P. Nikolopoulos, Wettability and Interfacial Interactions in Bioceramic-Body-Liquid Systems, *J. Biomed. Mater. Res.*, 1995, **29**, 421–429.
15 M. Mantel and J. P. Wightman, Influence of the surface Chemistry on the Wettability of Stainless Steel, *Surf. Interface Anal.*, 1994, **21**, 595–605.
16 L. Boulange-Petermann, C. Gabet and B. Baroux, On the respective effect of the surface energy and micro-geometry in the cleaning ability of bare and coated steels, *Colloids Surf., A*, 2006, **272**, 56–62.
17 H. P. Jennissen, Ultra-hydrophilic transition metals as histophilic biomaterials, *Macromol. Symp.*, 2005, **225**, 43–69.
18 O. Santos, T. Nylander, R. Rosmaninho, G. Rizzo, S. Yiantsios, N. Andritsos, A. Karabelas, H. Muller-Steinhagen, L. Melo, L. Boulange-Petermann, C. Gabet, A. Braem, C. Tragardh and M. Paulsson, Modified stainless steel surfaces targeted to reduce fouling - surface characterization, *J. Food Eng.*, 2004, **64**(1), 63–79.
19 A. Bhuyan, B. Gregory, H. Lei, S. Y. Yee, Y. B. Gianchandani, "Pulsed and DC electropolishing of stainless steel for stents and other devices", *Proc. IEEE Conf. Sensors*, Irvine, CA, 2005, pp. 314–7.
20 P. N. Brett, T. J. Parker, A. J. Harrison, T. A. Thomas and A. Carr, Simulation of resistance forces acting on surgical needles, *Proc. Inst. Mech. Eng., Part H*, 1997, **211**(4), 335–347.
21 H. Saito, K. Mitsubayashi and T. Togawa, Detection of needle puncture to blood vessel by using electric conductivity of blood for automatic blood sampling, *Sens. Actuators, A*, 2006, **125**, 446–450.
22 L. Azzi, M. El-Alfy, C. Martel and F. Labrie, Gender differences in mouse skin morphology and specific effects of sex steroids and Dehydroepiandrosterone, *J. Invest. Dermatol.*, 2005, **124**(1), 22–27.
23 O. A. Shergold and N. A. Fleck, Experimental investigation into the deep penetration of soft solids by sharp and blunt punches, with application to the piercing of skin, *J. Biomech. Eng.*, 2005, **127**(5), 838–848.
24 Normal *vs.* Diet Mouse, http://www.williams.edu/Biology/Faculty_Staff/sswoap/site/mousedietpic.htm.
25 M. Agah, K. D. Wise, "A fully-dry PECVD-oxynitride process for microGC column fabrication", *Proc. IEEE Int. Conf. Micro Electro Mechanical Systems (MEMS 2005)*, Miami Beach, FL, Jan. 2005, pp. 774–777.
26 J. Yoshida, "Microfluidic devices and microflow systems," *Flash Chemistry: Fast Organic Synthesis in Microsystems*, John Wiley & Sons, 2008.
27 K. Takahata and Y. B. Gianchandani, Batch mode micro-electro-discharge machining, *J. Microelectromech. Syst.*, 2002, **11**(2), 102–110.